

Optical fiber probe spectroscopy for laparoscopic monitoring of tissue oxygenation during esophagectomies

Daniel S. Gareau

Frederic Truffer

Oregon Health and Science University
Department of Biomedical Engineering
3303 SW Bond Avenue
Portland, Oregon 97239

Kyle Perry

Thai Pham

C. Kristian Enestvedt

James Dolan

John G. Hunter

Oregon Health and Science University
Department of Surgery
3181 SW Sam Jackson Park Rd
Portland, Oregon 97239

Steven L. Jacques

Oregon Health and Science University
Department of Biomedical Engineering
3303 SW Bond Avenue
Portland, Oregon 97239

Abstract. Anastomotic complication is a major morbidity associated with esophagectomy. Gastric ischemia after conduit creation contributes to anastomotic complications, but a reliable method to assess oxygenation in the gastric conduit is lacking. We hypothesize that fiber optic spectroscopy can reliably assess conduit oxygenation, and that intraoperative gastric ischemia will correlate with the development of anastomotic complications. A simple optical fiber probe spectrometer is designed for nondestructive laparoscopic measurement of blood content and hemoglobin oxygen saturation in the stomach tissue microvasculature during human esophagectomies. In 22 patients, the probe measured the light transport in stomach tissue between two fibers spaced 3-mm apart (500- to 650-nm wavelength range). The stomach tissue site of measurement becomes the site of a gastroesophageal anastomosis following excision of the cancerous esophagus and surgical ligation of two of the three gastric arteries that provide blood perfusion to the anastomosis. Measurements are made at each of five steps throughout the surgery. The resting baseline saturation is 0.51 ± 0.15 and decreases to 0.35 ± 0.20 with ligation. Seven patients develop anastomotic complications, and a decreased saturation at either of the last two steps (completion of conduit and completion of anastomosis) is predictive of complication with a sensitivity of 0.71 when the specificity equaled 0.71. © 2010 Society of Photo-Optical Instrumentation Engineers. [DOI: 10.1117/1.3512149]

Keywords: diffuse reflectance spectroscopy; optical fibers; oxygen saturation; surgery.

Paper 10097LSSRR received Feb. 24, 2010; revised manuscript received Sep. 30, 2010; accepted for publication Oct. 11, 2010; published online Nov. 19, 2010.

1 Introduction

A spectroscopic method¹ of assessing the oxygenation status of tissue was adapted using a simple two-optical-fiber probe suitable for use via laparoscopy. In contrast to pulse oximetry,²⁻⁵ which measures arterial blood oxygenation, and Doppler flowmetry,⁶⁻⁸ which measures a combination of blood volume and blood flow velocity, this steady-state measurement separately measures the blood volume fraction (B) and hemoglobin oxygenation (S) in the mixed arteriovenous microvasculature, and B and S together characterize the oxygen content in the tissue.

The near-infrared wavelength has been used^{9,10} for sampling with deep probing (>1 cm), but in this work, we tested shallow (<5 mm) monitoring of tissue oxygenation during human esophagectomy,¹¹ which is the surgical procedure of removal of a cancerous esophagus and restoration of gastrointestinal continuity with part of the stomach that is remodeled to serve as a gastric conduit tube. To mobilize the stomach tissue that will become the conduit, the tethering short gastric and left gastric arteries must be surgically ligated. The right gastroepiploic artery is the sole remaining vessel supplying the gastric conduit, and

consequently the blood supply is decreased to the very tissue that must be anastomosed to the remaining esophagus in the patient's neck. Ischemia is known to impact the occurrence rates of the two types of complications that can result in this surgery: 1. stricture, which can be treated postsurgically, and 2. anastomotic failure/leak, which leads to sepsis, a far more dangerous complication.

Anastomotic failure requires surgical intervention to fix leakage at the anastomosis connecting the gastric conduit to the pharynx. Postmortem examination of gastric conduits in post-esophagectomy patients showed that the blood supply of the proximal 20% of the gastric conduit was through a microscopic network of capillaries and arterioles.¹² Ischemia of the gastric conduit due to altered arterial inflow and venous drainage has been implicated in high anastomotic leak rates.¹²⁻¹⁷ Karl et al.¹⁸ reported that the incidence of anastomotic leak ranges between 3.5 and 19%. Similar results¹⁹ report 4.2% for anastomosis in the thoracic region and 15.5% for the cervical region. Many factors influence the outcome, but adequate oxygenation at the anastomosis is critical to success. Anastomosis strength has been correlated with oxygen by Karliczek et al.,²⁰ who showed that partially ischemic anastomoses had diminished breaking strength.

Address all correspondence to: Steven Jacques, CH13B Oregon Health and Science University, 3303 SW Bond Ave., Portland, OR, 97239. Tel: 503-708-7078; E-mail: jacquess@ohsu.edu.

There is currently no commercial means to monitor oxygenation of the anastomosis. Anastomotic leaks present too late for effective preventative intervention. Anastomotic leak contributes substantially to the 5% mortality¹¹ rate associated with esophagectomy, therefore any method of early detection for the scheduling of prefailure intervention would improve patient outcome. Detection of a significant decrease in normal tissue oxygenation at the anastomosis could alert the surgeon that the conduit or anastomosis may be at risk for ischemic injury, and further diagnostic and therapeutic intervention must be scheduled. This probe system contributes to the movement of steady-state optical spectroscopy^{21–26} into clinical practice.^{9, 10, 27–29}

Fiber optic spectroscopy can be implemented with a small footprint (two 1-mm-diam optical fibers placed 3 mm apart) and can avoid the dangers of placing electrical components in the patient. The probe measures a strong steady-state light signal, as opposed to a pulse oximetry unit³ that must lock onto a weak pulsatile signal to extract information. The oxyhemoglobin (HbO₂) and deoxyhemoglobin (Hb) molecules exhibit distinct absorption properties in the visible spectral range. The spectroscopic analysis utilizes the absorption spectra of oxy- and deoxyhemoglobin and optical diffusion theory, incorporating the tissue scattering properties and blood absorption to estimate the blood volume fraction (B) and the oxygen saturation of hemoglobin [$S = \text{HbO}_2/(\text{Hb} + \text{HbO}_2)$] in the mixed arteriovenous microvasculature.

2 Materials and Methods

Fiberoptic probes were prepared for sterile, one-time use on patients using standard machining and fiber polishing tools. The clear, 8-mm-diam cylindrical probe tip had 1-mm-diam holes drilled parallel to its axis at a separation distance of about 3 mm. Plastic fibers (NT02–534, Edmund Optics, Barrington, New Jersey) were used for flexibility and safety. The delivery fiber and a second identical fiber for light collection were polished along with the probe tip face to achieve one clear planar surface. Because the probes were hand-made, the separation distance varied from $r = 2.5$ to 3.5 mm, and for each probe this fiber separation was measured and cataloged for use in subsequent spectral analysis. In the operating room, two sterile 4-m-long fibers delivered and collected light between the surgeons and the “scrubbed in” engineer outside of the surgical sterile zone.

A white light source (HL-2000-LL, Ocean Optics, Dunedin, Florida) was coupled to the plastic fiber with a standard SMA connector (11040A, Thor Labs, Newton, New Jersey). A thin glass fiber of 100- μm core diameter (BFL22–200, Thor Labs, Newton, New Jersey) was coupled between the collection fiber and the spectrometer (QE 65000 using the OOI Base32 Spectrometer Software, Ocean Optics, Dunedin, Florida), which improved the resolution of the spectrometer. The spectrometer was controlled by a laptop computer (Dell Computer, Round Rock, Texas) running the Windows XP Professional operating system. The wavelength response of the probe depended on the wavelength dependence of the light source $S(\lambda)$ [W], and of the detector $D(\lambda)$ [counts/W]. Measured spectra of tissue were normalized by a measured spectrum of a white standard while holding the fiber a 3 cm from the standard, yielding the

measurement M in Eq. (1):

$$\begin{aligned} M &= \frac{S(\lambda)T_{\text{tissue}}A_{\text{det}}\eta_{\text{tissue}}D(\lambda)}{S(\lambda)R_{\text{std}}\eta_{\text{std}}D(\lambda)} \\ &= T_{\text{tissue}}\frac{A_{\text{det}}\eta_{\text{tissue}}}{R_{\text{std}}\eta_{\text{std}}} = R_{\text{tissue}}\text{CALIB}, \end{aligned} \quad (1)$$

where T_{tissue} [cm^{-2}] is the transport of light between the two fibers within the tissue, A_{det} [cm^2] is the area of fiber collection, and η_{tissue} is the fraction of escaping light that enters the detector fiber within the solid angle of collection to be carried to the detector. Similarly, R_{std} is the reflectance from the standard ($R_{\text{std}} \approx 0.997$; SpectralonTM, Labsphere Incorporated, North Sutton, New Hampshire) and η_{std} is the fraction of reflectance collected by the detector fiber held 3 cm distant from the standard. Hence, the product $S(\lambda)D(\lambda)$ was canceled, while a wavelength independent calibration factor, $\text{CALIB} = A_{\text{det}}\eta_{\text{tissue}}/(R_{\text{std}}\eta_{\text{std}})$, remained such that $R_{\text{tissue}} = M/\text{CALIB}$.

The probe was introduced percutaneously into the abdominal cavity through a 10-mm-diam trocar, and placed on the gastroesophageal anastomosis by the surgeons using surgical forceps via a second trocar. Visualization was by endoscopy through a third trocar. The endoscope light was turned off for spectral measurements. Spectra were collected at five time points during the surgery: 1. a baseline value, 2. after division of the short gastric arteries, 3. after division of the left gastric artery, 4. after creation of the gastric conduit, and 5. after completion of the anastomosis. At each time point, five measurements were taken in rapid succession at each of three locations ($n = 15$, although sometimes the surgeon measured fewer sites) within 2 cm of a marking stitch that identified the measurement location on the caudal side of the anastomosis site during creation of the gastric conduit. The integration time for each measurement was about 200 ms, but was adjusted for each measurement to obtain adequate signal without saturation of the spectrometer. Each spectrum was recorded with its integration time, and subsequent data analysis used the counts per spectral bin divided by the integration time [counts/bin/s]. The placement of the probe by the surgeon was important for a reliable spectral measurement, and since the surgeon had only visual feedback on whether a successful placement had occurred, often several of the placements at one site were not reliable. Therefore, following spectral analysis (see next), the median of B and S values deduced from spectra were used for evaluation of tissue status, which rejected outliers and found the center of the cluster of measurements at a particular surgical step.

The spectra were analyzed in the range 500 to 650 nm by least squares fitting using `fminsearch()` in Matlab (Mathworks, Natick, Massachusetts), which is a multidimensional unconstrained nonlinear minimization (Nelder-Mead). The measurement M in Eq. (1) was simulated as M_{theory} by the expression:

$$M_{\text{theory}} = \text{CALIB} \text{ get } Rr(\mu_a, \mu'_s, r, n). \quad (2)$$

The least-squares fitting minimized the error parameter $\text{ERROR} = \text{sum}\{\log[M(\lambda)] - \log[M_{\text{theory}}(\lambda)]\}^2$. The function `getRr()` in Eq. (2) was based on the diffusion theory expression of Farrell, Patterson, and Wilson²² for flux escaping at a distance

Table 1 Median of ~15 measurements per subject of blood volume fraction (B) and hemoglobin oxygen saturation (S) at the anastomotic site after each surgical step (1 = baseline, 2 = short gastric arterial ligation, 3 = left gastric artery ligation, 4 = completion of the conduit, 5 = completion of anastomosis) The 16 patients with no post-surgery complications, and the seven patients with postsurgical complications are listed. (NA = measurement not available.)

No complications:									
Step 1		Step 2		Step 3		Step 4		Step 5	
B	S	B	S	B	S	B	S	B	S
0.0184	0.458	NA	NA	0.0151	0.231	0.0132	0.229	0.0224	0.528
NA	NA	0.0088	0.556	0.0141	0.489	0.0160	0.408	0.0212	0.463
NA	NA	0.0140	0.482	0.0147	0.439	0.0131	0.450	0.0300	0.630
NA	NA	0.0081	0.641	0.0051	0.448	0.0123	0.516	0.0179	0.556
NA	NA	0.0133	0.497	0.0127	0.547	NA	NA	0.0163	0.511
NA	NA	0.0064	0.149	0.0098	0.196	0.0082	0.131	0.0086	0.635
NA	NA	0.0224	0.521	0.0183	0.480	0.0149	0.420	0.0214	0.464
0.0123	0.555	0.0144	0.554	0.0208	0.332	0.0153	0.291	0.0275	0.352
0.0075	0.570	0.0108	0.510	0.0088	0.511	NA	NA	0.0217	0.606
0.0163	0.475	0.0147	0.359	0.0111	0.311	0.0199	0.135	0.0297	0.214
0.0108	0.517	0.0101	0.520	0.0110	0.470	0.0106	0.227	0.0158	0.488
0.0033	0.337	0.0252	0.648	0.0139	0.758	0.0126	0.699	0.0290	0.574
NA	NA	0.0100	0.672	0.0122	0.696	0.0128	0.699	0.0109	0.649
NA	NA	0.0244	0.358	0.0082	0.237	0.0245	0.548	0.0059	0.238
0.0223	0.612	0.0244	0.173	0.0303	0.640	0.0370	0.618	0.0214	0.577
0.0120	0.139	NA	NA	0.0218	0.190	0.0182	0.525	0.0159	0.559
Complications									
0.0119	0.562	0.0135	0.436	0.0138	0.495	0.0119	0.176	0.0123	0.503
0.0082	0.661	0.0168	0.560	0.0139	0.406	0.0131	0.178	0.0048	0.701
0.0164	0.616	0.0110	0.688	0.0112	0.532	0.0151	0.133	0.0183	0.442
NA	NA	0.0062	0.464	0.0099	0.429	0.0058	0.059	0.0233	0.372
0.0081	0.610	0.0080	0.495	0.0067	0.375	0.0118	0.490	0.0213	0.491
NA	NA	0.0109	0.523	0.0164	0.455	0.0145	0.332	0.0199	0.396

r from a source fiber when placed topically on a tissue. The fiber separation was $r \approx 0.3$ cm (adjusted to the actual r of each constructed probe), and the refractive index mismatch between plastic and tissue was assumed to be $n = 1.10$. Equation (2) required the absorption coefficient μ_a [cm^{-1}] and the reduced scattering coefficient μ'_s [cm^{-1}], discussed later. The use of this analytical expression was valid, since the 3-mm source-detector separation was large compared to the transport mean free path [$1/(\mu_a + \mu'_s) = 1.26$ mm at 630 nm], and the reduced scattering dominated over the absorption.

The absorption coefficient of the tissue was specified:

$$\mu_a = B(S\mu_{a,\text{oxy}} + (1 - S)\mu_{a,\text{deoxy}}) + W\mu_{a,\text{water}}, \quad (3)$$

where B is the volume fraction of whole blood ($B = 1$ specifies 150-g hemoglobin/liter), S is the oxygen saturation of hemoglobin in the mixed arteriovenous vasculature, and W is the tissue water content. The terms $\mu_{a,\text{oxy}}$, $\mu_{a,\text{deoxy}}$ and $\mu_{a,\text{water}}$ are the absorption spectra for oxygenated whole blood, deoxygenated whole blood, and water, respectively.^{30,31} In the spectral fitting region of 500 to 650 nm, absorption due to water is

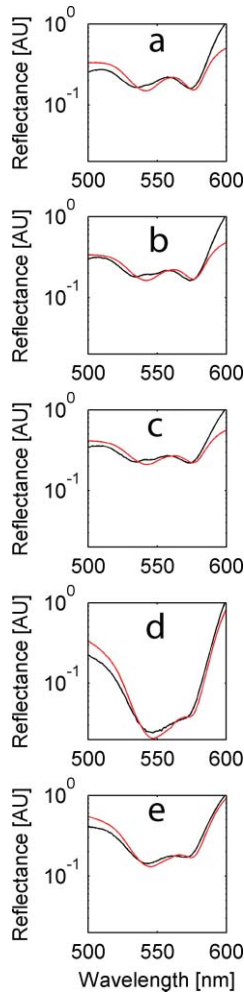


Fig. 1 Sample spectra for one patient through the surgical steps: (a) baseline measurement $S = 0.77$, $B = 0.010$, (b) short gastric arterial ligation $S = 0.70$, $B = 0.010$, (c) left gastric artery ligation $S = 0.68$, $B = 0.009$, (d) conduit completion $S = 0.28$, $B = 0.038$, and (e) anastomosis completion $S = 0.37$, $B = 0.020$.

negligible. At 650 nm, the absorption coefficient due to blood is 0.056 cm^{-1} , which is the value of $BS\mu_{a,\text{oxy}} + B(1-S)\mu_{a,\text{deoxy}}$, where $B = 0.010$ and $S = 0.50$. The μ_a due to water is 12-fold lower at 0.0045 cm^{-1} , which is the value of $W\mu_{a,\text{water}}$, where, $W = 0.75$. The reduced scattering coefficient of the tissue was assumed to behave as:

$$\mu'_s = \mu'_{s,630\text{nm}} \left(\frac{\lambda}{630 \text{ nm}} \right)^{-b}, \quad (4)$$

where $\mu'_{s,630\text{nm}}$ was the value of μ'_s at 630 nm, and the factor b characterized the wavelength dependence of scattering. The parameters $\mu'_{s,630\text{nm}}$ and b were assigned the value 7.7 cm^{-1} and 1.4 , respectively, based on Table 1 in Bargo et al.,³² who studied esophageal mucosa in nine normal patients and found values of 7.74 cm^{-1} and 1.42 , respectively. Li et al.³³ reported data for muscle that yields values of 7.57 cm^{-1} and 1.35 , respectively. Any error in the choice of $\mu'_{s,630\text{nm}}$ yields error in the deduced values of B , and S . For the mean values of $B = 0.0151$ and $S = 0.453$ observed in this study, and using $\mu'_{s,630\text{nm}}$ equal to 7.7 cm^{-1} and $b = 1.4$, the variation in B and S for an error in $\mu'_{s,630\text{nm}}$ can be estimated. For B , $(100\%)(\partial B/\partial \mu'_{s,630\text{nm}})/B = -9.9 \text{ [%/cm}^{-1}]$. For S , $(100\%)(\partial S/\partial \mu'_{s,630\text{nm}})/S = 6.1 \text{ [%/cm}^{-1}]$. While future work will establish the values of $\mu'_{s,630\text{nm}}$ and b for the *in-vivo* gastric sites of anastomosis, and improve the accuracy of absolute values of B and S , any error in the assumed values does not affect the relative changes seen in this study.

A total of 1439 spectra were acquired, and 1063 spectra were accepted as good on the basis of the least-squares fitting convergence, and the parameter ERROR was below a threshold value appropriate for excluding obvious outliers. The means and standard deviations for the fitted parameters for all the accepted spectra were $B = 0.0151 \pm 0.0067$ and $S = 0.453 \pm 0.162$, for $n = 100$ median values on sites from 23 subjects and five surgical steps.

Table 2 Mean Values \pm standard deviations for the grouped median measurements at the surgical steps shown in Table 1. Statistical significance is denoted by bold p values, as determined with a 1-tailed student T-test assuming unequal variance. The top section (A) expresses the raw data, in while the lower section (B) expresses the data as a fraction of the baseline value for only the patients with baseline measurements.

Stage	Tissue O ₂ saturation (S)		p value	Blood volume fraction (B)		p value
	No complication	Complication		No complication	Complication	
A:step 2	0.474 ± 0.162	0.524 ± 0.083	0.184	0.015 ± 0.007	0.011 ± 0.004	0.045
A:step 3	0.436 ± 0.176	0.448 ± 0.053	0.402	0.014 ± 0.006	0.012 ± 0.003	0.146
A:step 4	0.421 ± 0.194	0.210 ± 0.151	0.007	0.016 ± 0.007	0.012 ± 0.003	0.048
A:step 5	0.503 ± 0.132	0.482 ± 0.108	0.346	0.020 ± 0.007	0.019 ± 0.010	0.430
B:step 2	0.994 ± 0.600	0.888 ± 0.155	0.24	2.34 ± 2.95	1.21 ± 0.59	0.102
B:step 3	1.091 ± 0.674	0.744 ± 0.150	0.073	1.79 ± 1.40	1.09 ± 0.44	0.075
B:step 4	0.867 ± 0.729	0.400 ± 0.271	0.045	1.78 ± 1.16	1.24 ± 0.33	0.090
B:step 5	0.936 ± 0.479	0.870 ± 0.146	0.286	3.05 ± 3.23	1.34 ± 0.89	0.062

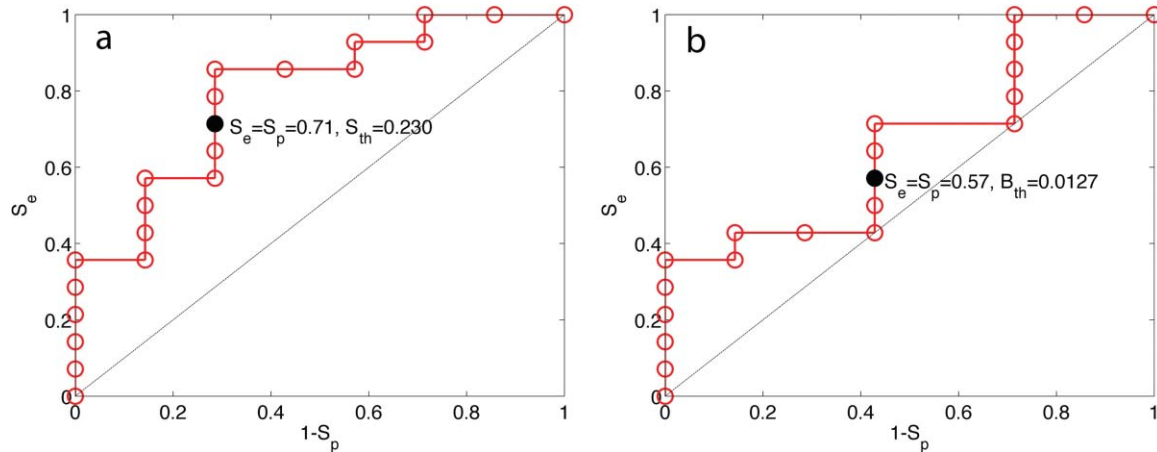


Fig. 2 The sensitive (S_e) and specificity (S_p) of predicting complications. (a) S_e versus $1-S_p$ based on the oxygen saturation (S) dropping below a threshold S_{th} at either the completion of the conduit (surgical step 4) or the completion of the anastomosis (surgical step 5). The threshold value of S used as a discriminator (S_{th}) was increased in incremental steps, and the data at $S_{th} = 0.230$ are shown as a solid circle. (b) The S_e versus $1-S_p$ based on the blood content (B) dropping below a threshold B_{th} at either surgical step 4 or 5 yields $S_e = S_p = 0.57$ when $S_{th} = 0.0127$.

3 Results

Table 1 shows the statistics for accepted data for each time point during the surgery. There was a progressive drop in S and rise in B , until the anastomosis was completed. Figure 1 shows a sample spectrum from each surgical step where the saturation followed the typical trend. In general, after the first step (division of short gastric arteries), S dropped slightly, but B remained constant. The subsequent steps (division of left gastric artery, creation of conduit) caused a further and larger drop in S and rise in B . After completion of the anastomosis, S recovered partially but B remained high. Compared to patients without anastomotic complications, those who manifested anastomotic complications had greater intraoperative changes in S and B . Table 2 shows the statistically significant p values of less than 0.05 for such complications that exhibited low blood volume fractions at step 2, and poor oxygen saturation as well as low blood volume fractions at step 4.

There were complications, either leakage or strictures, in 7 of the 23 subjects. A threshold value S_{th} was chosen for the minimum value of oxygen saturation (S) at either the completion of the conduit (surgical step 4) or the completion of the anastomosis (surgical step 5). If the mean value of S for either surgical step dropped below S_{th} , a complication was predicted. Figure 2(a) is a receiver-operator curve (ROC) that shows the sensitivity (S_e) and specificity (S_p) for predicting complications using different values of S_{th} . The $S_e = S_p = 0.71$ when $S_{th} = 0.230$. Figure 2(b) shows a similar ROC using a threshold blood content B_{th} as the discriminator, yielding $S_e = S_p = 0.57$ when $S_{th} = 0.0127$.

4 Discussion

While the number of patients tested and complications arising are still low, the preliminary data suggest that tissue oxygen saturation (S) may identify when the anastomoses is at risk for complications. Blood content (B) is less predictive, but can also contribute to assessing risk. Flagging patients at risk for extra

attention in postoperative care should prove useful in patient management.

Acknowledgments

This work was supported in part by the Oregon Clinical and Translational Research Institute (OCTRI) and in part by the National Institutes of Health, USA (NIH RO1-HL084013). Dan Gareau is supported by an NIH National Research Service Award (NIH 5-T32-CA106195, PI: Molly Kulesz-Martin).

References

1. D. A. Benaron, I. H. Parachikov, W. F. Cheong, S. Friedland, B. E. Rubinsky, F. W. H. Liu, C. J. Levinson, A. L. Murphy, J. W. Price, Y. Talmi, J. P. Weersing, J. L. Duckworth, U. B. Hörtchner, and E. L. Kermit, "Design of a visible-light spectroscopy clinical tissue oximeter," *J. Biomed. Opt.* **10**(4), 044005 (2005).
2. T. L. Rusch, R. Sankar, and J. E. Scharf, "Signal processing methods for pulse oxymetry," *Comput. Biol. Med.* **26**, 143–159 (1996).
3. M. N. Ericson, M. A. Wilson, G. L. Cote, J. S. Baba, W. Xu, M. Bobrek, C. L. Britton, M. S. Hileman, M. R. Moore, M. S. Emery, and R. Lenarduzzi, "Implantable sensor for blood flow monitoring after transplant surgery," *Min. Invas. Ther. Appl. Technol.* **13**(2), 87–94 (2004).
4. M. Yelderian and W. New, "Evaluation of pulse oxymetry," *Anesthesiol.* **59**(4), 349–352 (1983).
5. V. Kamat, "Pulse Oximetry," *Indian J. Anaesth.* **46**(4), 261–268 (2002).
6. G. M. D. Michelson, B. Schmauss, M. J. Langhans, J. Harazny, and M. J. Groh, "Principle, validity, and reliability of scanning laser Doppler flowmetry," *J. Glaucoma* **5**(2), 99–105 (1996).
7. P. Wellhöner, D. Rolle, P. Lönnroth, L. Strindberg, M. Elam, and C. Dodi, "Laser-Doppler flowmetry reveals rapid perfusion changes in adipose tissue of lean and obese females," *Am. J. Physiol. Endocrinol. Metab.* **291**, E1025-E1030 (2006).
8. T. Miyazaki, H. Kuwano, H. Kato, M. Yoshikawa, H. Ojima, and K. Tsukada, "Predictive value of blood flow in the gastric tube in anastomotic insufficiency after thoracic esophagectomy," *World J. Surg.* **26**, 1319–1323 (2002).
9. F. Jobsis, "Noninvasive infrared monitoring of cerebral and myocardial sufficiency and circulatory parameters," *Sci. Wash.* **198**, 1264–1267 (1977).
10. J. S. Wyatt, M. Cope, D. T. Delpy, C. E. Richardson, A. D. Edwards, S. Wray, and E. O. R. Reynolds, "Quantitation of cerebral blood volume in human infants by near-infrared spectroscopy," *J. Appl. Physiol.* **68**, 1086–1091 (1990).

11. M. B. Orringer, B. Marshall, and M. C. Stirling, "Transhiatal esophagectomy for benign and malignant disease," *J. Thorac. Cardio. Surg.* **105**, 265–276 (1993).
12. D. M. I. Liebermann-Meffert, R. Meier, and J. R. Siewert, "Vascular anatomy of the gastric tube used for esophageal reconstruction," *Ann. Thorac. Surg.* **54**, 1110–1115 (1992).
13. J. P. Pierie, P. W. De Graaf, H. Poen, I. Van Der Twel, and H. Obertop, "Impaired healing of cervical esophagogastronomies can be predicted by estimation of gastric serosal blood perfusion by laser Doppler flowmetry," *Eur. J. Surg.* **160**, 599–603 (1994).
14. J. D. Urschel, "Esophagogastronomy anastomotic leaks complicating esophagectomy: a review," *Am. J. Surg.* **169**, 634–640 (1995).
15. N. H. Boyle, A. Pearce, D. Hunter, W. J. Owen, and R. C. Mason, "Scanning laser Doppler flowmetry and intraluminal recirculating gas tonometry in the assessment of gastric and jejunal perfusion during oesophageal resection," *Br. J. Surg.* **85**, 1407–1411 (1998).
16. W. Schröder, D. Stippel, M. Lacher, C. Gutschow, and A. H. Hölscher, "Intraoperative changes of mucosal pCO₂ during gastric tube formation," *Langenbecks Arch. Surg.* **386**, 324–327 (2001).
17. W. Schröder, K. T. E. Beckurts, D. Stähler, H. Stützer, J. H. Fischer, and A. H. Hölscher, "Microcirculatory changes associated with gastric tube formation in the pig," *Eur. Surg. Res.* **34**, 411–417 (2002).
18. R. C. Karl, R. Schreiber, D. Boulware, S. Baker, and D. Coppola, "Factors affecting morbidity, mortality, and survival in patients undergoing Ivor Lewis esophagostrectomy," *Ann. Surg.* **231**(5), 635–643 (2000).
19. A. Turkyilmaz, A. Eroglu, Y. Aydin, C. Tekinbas, E. M. Muharrem, and N. Karaoglanoglu, "The management of esophagogastric anastomotic leak after esophagectomy for esophageal carcinoma," *Dis. Esophagus* **22**(2), 119–126 (2009, Epub 2008 Oct.1).
20. A. Karliczek, D. A. Benaron, C. J. Zeebregts, T. Wiggers, and G. M. van Dam, "Intraoperative ischemia of the distal end of colon anastomoses as detected with visible light spectroscopy causes reduction of anastomotic strength," *J. Surg. Res.* **152**(2), 288–95 (2009, Epub 2008 May 6).
21. S. A. Prahl, see <http://omlc.ogi.edu/spectra/hemoglobin/>, Oregon Medical Laser Center, Portland, OR (2009).
22. T.J. Farrell, M. S. Patterson, and B. C. Wilson, "A diffusion theory model of spatially resolved, steady-state diffuse reflectance for the non-invasive determination of tissue optical properties," *Med. Phys.* **19**, 879–888 (1992).
23. R. A. J. Groenhuis, H. A. Ferwerda, and J. J. Ten Bosch, "Scattering and absorption of turbid materials determined from reflection measurements. 2: measuring method and calibration," *Appl. Opt.* **22**(16), 2463–2467 (1983).
24. K. Ono, M. Kanda, J. Hiramoto, K. Yotsuya, and N. Sato, "Fiber optic reflectance spectrophotometry system for in vivo tissue diagnosis," *Appl. Opt.* **30**(1), 98–105 (1991).
25. G. A. Milikan, "An oximeter: an instrument for measuring continuously oxygen saturation of arterial blood in man," *Rev. Sci. Instrum.* **13**, 434–444 (1942).
26. C. D. Kurth and W. S. Thayer, "A multiwavelength frequency-domain near-infrared cerebral oximeter," *Phys. Med. Biol.* **44**(3), 727–740 (1999).
27. C. E. Elwell, S. J. Matcher, L. Tyszczuk, J. H. Meek, and D. T. Delpy, "Measurement of cerebral venous saturation in adults using near infrared spectroscopy," *Adv. Exp. Med. Biol.* **411**, 453–460 (1997).
28. V. Quaresima, S. Sacco, R. Totaro, and M. Ferrari, "Noninvasive measurement of cerebral hemoglobin oxygen saturation using two near infrared spectroscopy approaches," *J. Biomed. Opt.* **5**(2), 201–205(2000).
29. W. N. Colier, N. J. van Haaren, and B. Oeseburg, "A comparative study of two near infrared spectrophotometers for the assessment of cerebral haemodynamics," *Acta Anaesthesiol. Scand., Suppl.* **107**, 101–105 (1995).
30. W. B. Graetzer and N. Kollias, Personal communication, see <http://omlc.ogi.edu/spectra/hemoglobin/summary.html> (1999).
31. G. M. Hale and M. R. Querry, "Optical constants of water in the 200nm to 200 μ m wavelength region," *Appl. Opt.* **12**, 555–563 (1973).
32. P. R. Bargo, S. A. Prahl, T. T. Goodell, R. A. Slevin, G. Koval, G. Blair, and S. L. Jacques, "In vivo determination of optical properties of normal and tumor tissue with white light reflectance and an empirical light transport model during endoscopy," *J. Biomed. Opt.* **10**(3), 034018 (2005).
33. A. Li, R. Kwong, A. Cerussi, S. Merritt, C. Hayakawa, and B. Tromberg, "Method for recovering quantitative broadband diffuse optical spectra from layered media," *Appl. Opt.* **46**(21), 4828–4833 (2007).